ON THE OPERATION MECHANISM OF A POROUS HYDROGEN ELECTRODE WITH A NICKEL CATALYST

R.Ch.Burshtein, A.G.Pshenichnikov, F.Z.Sabirov
Institute of Electrochemistry, Academy of Sciences of the USSR, Moscow.

It follows from our previous investigations of the operation mechanism of porous gas electrodes [1-3] that a porous electrode can be represented by a model shown in Fig.1. In Bacon's two-layer electrodes the fine pore layer practically does not participate in the electrochemical process. Electrochemical processes occur only in the layer of the electrode, which consists of two kinds of pores: macropores and micropores. Micropores are filled with electrolyte and macropores with gas. Electrochemical reaction occurs on the walls of macropores covered with a thin electrolyte film. The thickness of the electrolyte film determined from the data for a half-immersed nickel electrode is 0,5-1μ [4]. We used such a model of the porous electrode in the preparation of active electrodes for a hydrogen-oxygen cell.

According to Justi, active metalloceramic hydrogen electrodes can be prepared using nickel skeleton catalyst [5].

It should be noted that the preparation of electrodes by the Justi method requires a very long time because the aluminium elimination process occurs extremely slowly. These electrodes do not posess sufficient mechanical strength and operate steadily for a long period of time only at small current densities 30-50 ma/cm^2 [5].

We have developed a method of preparing hydrogen electrodes using a skeleton nickel catalyst, obtained from an alloy containing 50% Ni, 48% Al and 2% Ti [6].

It is known that such catalyst has larger catalytic activity and stability than the usual Raney catalyst. The influence of the heating temperature in hydrogen upon the specific surface of a catalyst containing a Ti addition was investigated. It was shown that the specific surface of a powder, measured by the BET method, remained practically unchanged upon heating in hydrogen up to 800°C and was equal to 80-90 m^2/g.

Electrodes were prepared as follows. The alloy previously ground in a vibrating mill and the powder obtained was freed of aluminium by treating with 5 N KOH. Such catalyst is highly pyrophoric, but when mixed in the wet state with carbonyl nickel, it loses this property and such a mixture can be stored dry a

long time. The loss of pyroforic properties by catalysts when they are mixed with carbonyl nickel is accounted for by the slow diffusion of oxygen through the water film and the formation of a thin oxide film on the catalyst surface. An investigation of the electrodes with varying structures activated by the skeleton catalyst carried out by the method similar to that used in [1].

In designing electrodes of large size of essential importance is the electrode strength. To ensure better strength a new design of electrodes with an internal gas feed was developed [7].

Such an electrode is shown schematically in Fig.2. The electrode consists of a shell made of readily sintering carbonyl nickel (edge - 1 and fine pore layer - 2) with the active layer - 3 inside (a mixture of skeleton catalyst and carbonyl nickel). Gas is supplied through side tubes - 4. In the case of the electrodes having 120 mm in diameter strengthening and gas-feed paths - 5 are used. Strength is ensured by the electrode edge and gas-feed paths, which sinter well with the fine pore layers. Such electrodes were pressed in a special die in one operation. Gas feed paths can be of different forms. The electrodes operate both sides. Their operating surface is 165 cm^2 (both sides). When assembling the cell the electrodes are placed into a tank with electrolyte and connected in parallel with respect to gas and current.

The dependence of the current J_a upon the potential for a three-layer electrode with α = 0,25 at different temperatures is given in Fig.3. Fig.4 shows the dependence of log J (at φ = 80 mv) upon the reciprocal temperature. The apparent activation energy of the process calculated from the slope of the straight line is 5 Cal/mol ^{o}C.

Tests on a large number of electrodes have shown good reproducibility of the results. The electrodes operated steadily in a hydrogen-oxygen cell for 12 months.

In the case of electrodes with high electrochemical activity the ohmic losses in the fine pore layer are large and therefore with a decrease in its thickness the current density increases. The experimental curve of the current density dependence upon the thickness of the fine pore layer is shown in Fig.5.

Of considerable interest is the dependence of the electrochemical activity of the electrode upon the skeleton catalyst content in the active mixture. As is evident from Table 1, with

an increasing ratio of the catalyst weight to that of the mixture (α) the current density rises up to $\alpha = 0,5$.

Table 1.

α	0	0,10	0,25	0,30	0,40	0,50	0,75	1,00
J ma/cm^2 (φ = 0,08 v)	50	108	140	151	168	185	136	108

With further increase in α (α = 0,75 and α = 1,00) the current density drops. As is shown by the structure measurements, it dependence on the change ratio of the macro- to micro pores. Of considerable interest in designing the three-layer electrodes is the dependence of the current density at a constant potential upon the active layer thickness. This dependence is shown in Fig.6. It is evident from the figure that at the thicknesses less than 1,5 mm the current density considerably decreases.

Now let us consider how the concepts of the porous electrode operation developed in [1-3] can be applied to the electrode activated with a skeleton catalyst.

The J - φ dependences of the electrodes in question being linear at small polarization (see Fig.3), the electrode resistance R can be considered to be determined by the relation:

$$R = \varphi / J = r_a + r_f \qquad \ldots (1)$$

where r_a is the active layer resistance, r_f - the fine pore layer resistance. The fine pore layer resistance is expressed by the equation:

$$r_f = \rho \cdot \xi^2 \delta / v_f \qquad \ldots (2)$$

where ρ - is the electrolyte specific resistance, ξ - the sinuosity coefficient, v_f - total cross-section of the pores in the fine pore layer per unit of visible surface, equal to the fine pore layer porosity. In most cases $\xi = \sqrt{3}$ [8].

Now let us consider the dependence of the reaction resistance r_a upon the electrode activity.

According to (2), the dependence of the current density upon the gas electrode parameters is of the form:

$$J = (1/\xi) \sqrt{\lambda / \rho} \cdot \sqrt{P \Phi} \cdot \varphi \qquad \ldots (3)$$

where P is the total perimeter of the pores free of the electrolyte, Φ - the total cross-section of the pores filled with the electrolyte, $\lambda = \left(\frac{di}{d\varphi}\right)_{\varphi=0} \cdot \chi$, where i is the local

current density, χ - the ratio of the true to the visible surface. Let us assume that to the first approximation χ is proportional to the specific surface of the active mixture S_a. It is evident that in the mixture of the catalyst with carbonyl nickel.

$$S_a = \alpha \cdot S_{cat} + (1 - \alpha) \cdot S_{carb} \qquad \ldots (4)$$

The specific surface measurements using the BET method have shown the specific surface of the catalyst S_{cat}=80 m^2/gr, the specific surface of the carbonyl nickel powder S_{carb} = 0,55 m^2/gr.

According to the equations (3) and (4), for the electrodes with the same structure we obtain:

$$(r_c/r_a) = (S_a/S_{carb})^{1/2} = \left\{\alpha\left(S_{cat}/S_{carb} - 1\right)+1\right\} \qquad \ldots (5)$$

where r_c and r_a are the reaction resistances of the electrodes prepared from carbonyl nickel alone and from the active mixture, respectively.

Substituting the values of S_{cat} and S_{carb}, we obtain for the powdered catalyst used by us:

$$(r_c/r_a) = (144\alpha + 1)^{1/2} \qquad \ldots (6)$$

Substituting $r_c = \varphi/J$, obtained from equations (3) into (5) and using (2), we find for the total electrode resistance R the expression:

$$R = \frac{\left\{\alpha\left[\left(S_{cat}/S_{carb}\right) - 1\right] + 1\right\}^{1/2}}{(1/\xi)\,(\lambda_c/\rho)^{1/2}\,(P\Phi)^{1/2}} + \frac{\rho\xi^2}{v_f}\,\delta \qquad (7)$$

where $\lambda_c = \left(\partial i/\partial\varphi\right)_{\varphi\to 0}$ for a non-active electrode.

Assuming for a 7 N KOH at 90°C ρ = 0,715 ohm.cm [5] and taking the value of λ_c from [2], we obtain: $(1/\xi)\,(\lambda_c/\rho)^{1/2}$ = 0,024 $ohm^{-1} cm^{-3/2}$. It follows from the direct measurements of the fine pore layer porosity that v_f = 0,5. Substituting the values of ρ and ξ^2, we obtain for the coefficient before $\rho\xi^2/v_f$ = 4,25 ohm.cm. Taking into consideration (6), we obtain from (7) for the active nickel hydrogen electrode:

$$R = \frac{41,5}{(P\Phi)^{1/2}\,(144\alpha + 1)^{1/2}} + 4,3\,\delta \qquad \ldots (8)$$

where

$$r_a = \frac{41,5}{(P\Phi)^{1/2}\,(144\alpha + 1)^{1/2}} \qquad \ldots (8')$$

$$r_f = 4,3\,\delta \qquad \ldots (8'')$$

The relation $(P\Phi)^{1/2} = f(\Delta P)$ obtained from the pores distribution curve of the electrode with the structure investi-

gated by us $\alpha = 0,25$ is shown in Fig.7b. The fine pore layer thickness $\delta = 0,071$ cm. In accordance with the determination of R (1) and eq (8), for an electrode with the operating surface $S_e = 165$ cm^2 at $= 0,08$ v, the current is equal to:

$$J = \frac{S_e}{R} \cdot \varphi = \frac{165 \cdot 0,08}{\frac{41,5}{0,1} + 4,45 \cdot 0,071}, a \quad \ldots (8''')$$

Fig.7 shows the experimental (Curve 1) and the calculated (Curve 2) dependences of the current strength upon the pressure difference between gas and electrolyte. At large values of ΔP the calculation and experimental results can be considered to agree fairly well. At small ΔP the discrepancy appears to be due to the small gas permeability of the worse owing to some of the gas supplying canals.

Using eq (8) and (1) it is possible to calculate the dependence of the current J on an electrode upon the fine pore layer thickness. The results of the calculation and the comparison with the experimental data of Fig.5 are presented in Table 2.

Table 2.

δ cm	r_f ohm.cm^2	R ohm.cm^2	J, a $\Delta P = 600$ mm H $\varphi = 0,025$ v		$\varphi = 0,08$ v	
			calcul.	experim.	calcul.	experim.
0	0	0,32	12,9	-	41	-
0,01	0,042	0,36	11,2		37	
0,05	0,212	0,53	7,8	9,0	25	30
0,07	0,31	0,63	6,6	7,5	21	22
0,10	0,425	0,74	5,6	6,0	17	17

It is clear from the table that the agreement between the calculated and experimental values is quite satisfactory.

According to equation (8'), r_a decreases and hence the current increases with increasing skeleton catalyst content (α) in the active mixture.

The experimental results for the electrodes with identical structure but varying catalyst content (α) are given in Table 1. The values of R and r_a calculated from the data in Table 1 are listed in Table 3. Equation (6) relates the values obtained from the electrochemical and structure data for the electrodes with identical structures. The right hand and the left hand sides of equation (6) are given in Table 3 (columns 4 and 5). The comparison of the corresponding values shows that up to $\alpha = 0,5$ the experimental and calculated data agree with the accuracy up to

20%. The discrepancy between the data at $\alpha = 0,5$ is due, as stated above, to the change in the electrode structure.

Table 3.

α	R ohm.cm^2	r_a ohm.cm^2	$S_a/S_{carb.}$	r_c/r_a	$\Delta p = 600$mm L	Δ_{cr} mm
0	1,6	1,29	1	1,0	1,3	4,0
0,10	0,74	0,43	3,92	3,0	0,4	1,3
0,25	0,57	0,26	6,10	5,0	0,25	0,8
0,30	0,53	0,22	6,65	6,9	0,2	0,65
0,40	0,476	0,166	7,65	7,8	0,15	0,5
0,50	0,433	0,123	8,55	10,5	0,1	0,30
0,75	0,588	0,278	10,4	4,65		
1,00	0,74	0,43	12,0	3,0		

As has been shown in [2-3], the characteristic thickness is determined by the equation(9)

$$L = (1/\xi)\ (\varphi/\rho \cdot \rho\lambda)^{1/2} \qquad \ldots (9)$$

Using the obvious relation $\lambda_a = \lambda_c \cdot S_a/S_{carb.}$ and equation(5), we obtain for the electrodes with identical structure

$$L_c/L_a = (S_a/S_{carb.})^{1/2} = r_c/r_a \qquad \ldots (10)$$

where L_c and L_a are characteristic lengths of the nonactive and active electrodes, respectively.

According to [2-3], at the thickness $\ell < 1,6L$ the electrode can be considered to be of infinite thickness. For such electrodes the current density is determined by eq (3). Using eq (3) and (9) and taking into consideration (1), we obtain:

$$L = r_a \cdot \varphi/(\xi^2\rho) \qquad \ldots (11)$$

For the electrodes with the structure under consideration (NH_4HCO_3 240-340 mesh, 20%) at $\Delta p \sim 600$-900 mm Hg $\varphi \approx 0,2$ [2]. Then $L_a \approx 0,1 r_a$. The values of L thus calculated are given in column 6 of Table 3.

At $\ell \leq 1,6L$ [2-3] the current density is less than the maximum value determined from equation (3). The corresponding thickness Δ_{cr} of the three-layer electrode at which the current starts to decrease is $\Delta_{cr} = 2 \times 1,6L$. The values of Δ_{cr} are listed in column 7 of Table 3. For the electrodes with $\alpha = 0,25$ $\Delta_{cr} = 0,8$mm. According to Fig.6, the decrease in the activity on such an electrode occurs at $\Delta < 1,5$ mm, which appears to be due to a unsufficient gas distribution on the electrode.

Thus this concepts of the operation of the porous gas electrode can be used in the calculations and choice of the optimum conditions of operation of an active gas electrode. On the basis of the three-layer electrodes developed, it is possible to construct a cell of a simple design for a long time operation.

REFERENCES

1. R.Ch.Burshtein, A.G.Pshenichnikov, N.A.Shumilova, Dokl.Akad. Nauk SSSR, 143, 168 (1962).
2. A.G.Pshenichnikov, Dokl.Akad.Nauk SSSR, 148, 1121 (1963).
3. R.Ch.Burshtein, V.S.Markin, A.G.Pshenichnikov, Yu.A.Chizmadzhev, Yu.G.Chirkov, Electrochimica Acta, 9, 773 (1964).
4. A.G.Pshenichnikov, G.I.Shnaider, R.Ch.Burshtein, Elektrokhimiya, 1, 418 (1965).
5. E.Justi, A.Vinsel, Fuel Cells, Moscow, 1964.
6. A.G.Pshenichnikov, R.Ch.Burshtein, D.I.Lainer, Patent N147616, Sept.1961.
7. R.Ch.Burshtein, A.G.Pshenichnikov, N.A.Shumilova, Patent N 26596 of 10 Novemb.1961.
8. N.Bjerrum, E.Manegold, Koll.Z.,42, 97 (1927); 43, 5 (1927).

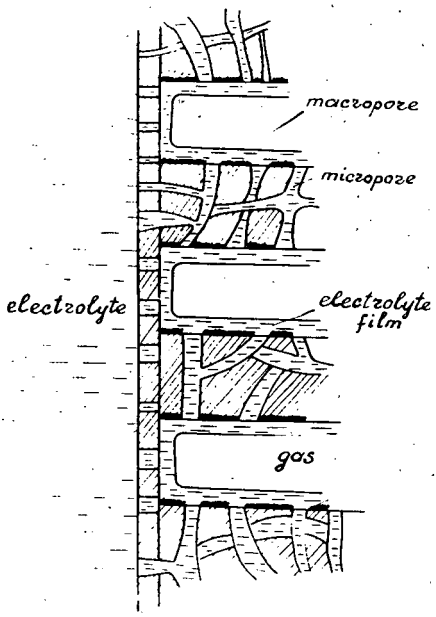

Fig.1. Porous gas electrode model.

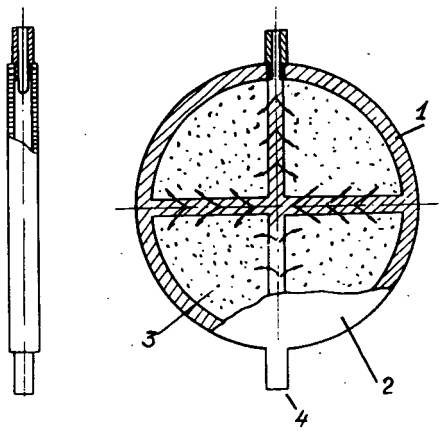

Fig.2. Scheme of an electrode with internal gas supply.

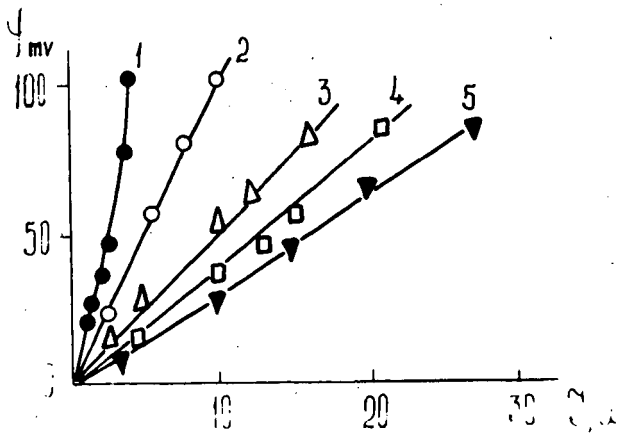

Fig.3. Polarization curves for different temperatures 1 - 20°, 2 - 40°, 3 - 60°, 4 - 77°, 5 - 92°.

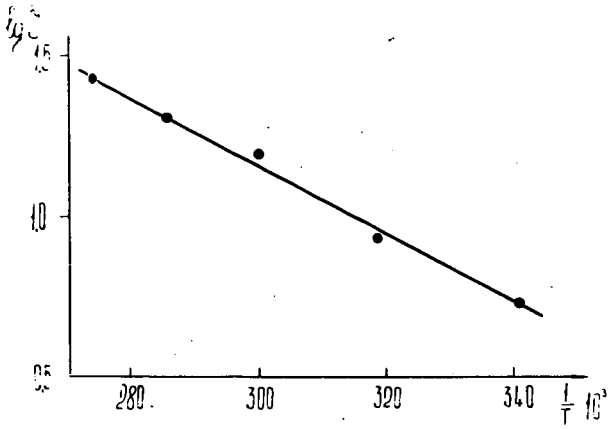

Fig.4. Dependence of lg J on 1/T . φ = 0,08 v.

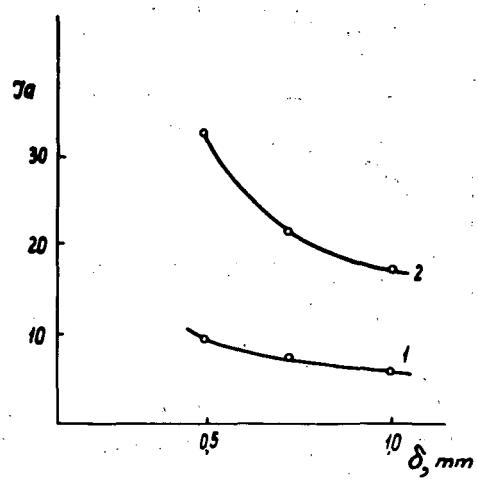

Fig.5. Dependence of J upon the fine pore layer thickness. 1 φ = 0,025 v. 2 - φ = 0,08 v.

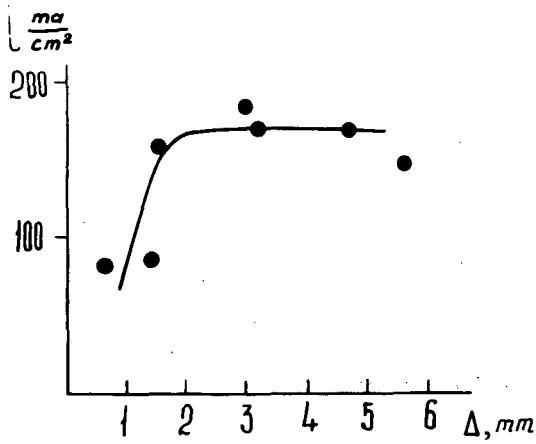

Fig.6. Dependence of current density upon the active layer thickness.

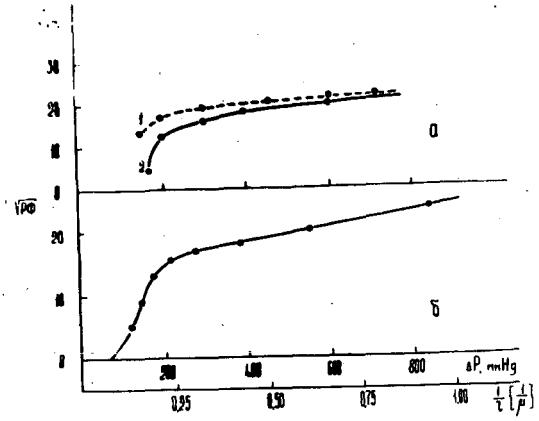

Fig.7. a - $J = f_1(\Delta P)$; $S_e = 165$ cm^2, $\varphi = 0{,}08$ v .
1 - calculation, 2 - experiment, b - $(P\varphi)^{1/2} = f_2(\Delta P)$.